DOI: 10.1002/chem.200802548

Rhodium(I)-Catalysed Intramolecular [2+2+2] Cyclotrimerisations of 15-, 20- and 25-Membered Azamacrocycles: Experimental and Theoretical Mechanistic Studies

Anna Dachs,[a] Anna Torrent,[b] Anna Roglans,*[b] Teodor Parella,[c] Sílvia Osuna,[a] and Miquel Solà*[a]

Dedicated to Professor Josep Font on the occasion of his 70th birthday

Abstract: A new series of 20- and 25-membered polyacetylenic azamacrocycles have been satisfactorily prepared and completely characterised by spectroscopic methods. Various [2+2+2] cyclotrimerisation processes catalysed by the Wilkinson's catalyst, [RhCl(PPh$_3$)$_3$], were tested in the above-mentioned macrocycles. The 25-membered azamacrocycle (like the previously synthesised 15-membered azamacrocyle) led to the expected cyclotrimerised compound in contrast to the 20-membered macrocycle, which is characterised by its lack of reactivity. The difference in reactivity of the 15-, 20- and 25-membered macrocycles has been rationalised through density functional theory calculations.

Keywords: cyclotrimerization · density functional calculations · macrocycles · reaction mechanisms · rhodium

Introduction

Transition-metal-catalysed [2+2+2] cyclotrimerisation reactions involving alkynes, in which three carbon–carbon bonds are formed in one step, is one of the most elegant methods for the construction of polysubstituted aromatics, which have important academic and industrial uses (for recent reviews see references [1–4]) The Wilkinson's complex [RhCl(PPh$_3$)$_3$] has been widely employed in these reactions. Partially intramolecular approaches or fully intramolecular cycloaddition processes represent efficient entries into various multiple-fused ring compounds. Over the last few years, we have developed an efficient rhodium(I)-catalysed [2+2+2] cyclotrimerisation process of 15-, 16- and 17-membered triynic and enediynic azamacrocycles of type **1** (to give compounds **2**) and have described the first examples in the literature of completed closed systems[5–8] (Scheme 1). To broad-

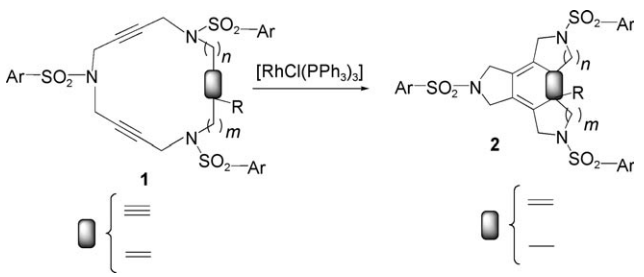

Scheme 1. Cyclotrimerisation reactions of macrocyclic triynes and enediynes.

[a] A. Dachs, S. Osuna, Prof. M. Solà
Institut de Química Computacional and
Departament de Química
Universitat de Girona
Campus de Montilivi, 17071 Girona (Spain)
Fax: (+34) 972-418-356
E-mail: miquel.sola@udg.edu

[b] A. Torrent, Dr. A. Roglans
Departament de Química
Universitat de Girona
Campus de Montilivi, 17071 Girona (Spain)
Fax: (+34) 972-418-150
E-mail: anna.roglans@udg.edu

[c] Dr. T. Parella
Servei de RMN
Universitat Autònoma de Barcelona
Cerdanyola, 08193 Barcelona (Spain)

Supporting information for this article is available on the WWW under http://dx.doi.org/10.1002/chem.200802548. It contains experimental description of all new compounds shown in Scheme 2 and ^{1}H and ^{13}C NMR spectra for compound **14** and details of the structure determination, including atomic coordinates, bond lengths and angles, thermal parameters, least-squares planes and interatomic contacts of macrocycle **3a**. Cartesian *xyz* coordinates and total energies of all stationary points located are also given.

en the scope of these cyclotrimerisation reactions to other macrocyclic systems and to afford new kind of fused tetracycles, we have prepared 20-membered tetraacetylenic azamacrocycles **3a–c** and 25-membered pentaacetylenic azamacrocycle **4** (Scheme 2) and studied their cyclotrimerisation reactions catalysed by the Wilkinson's complex.

Later in this paper, we shall discuss our finding that unlike the 15- and 25-membered azamacrocycles, the 20-membered tetraacetylenic azamacrocycles **3a–c** do not lead to the expected [2+2+2] cyclotrimerisation products. To understand the origin of this lack of reactivity, we decided to carry out theoretical calculations using density functional theory (DFT) with a hybrid functional.

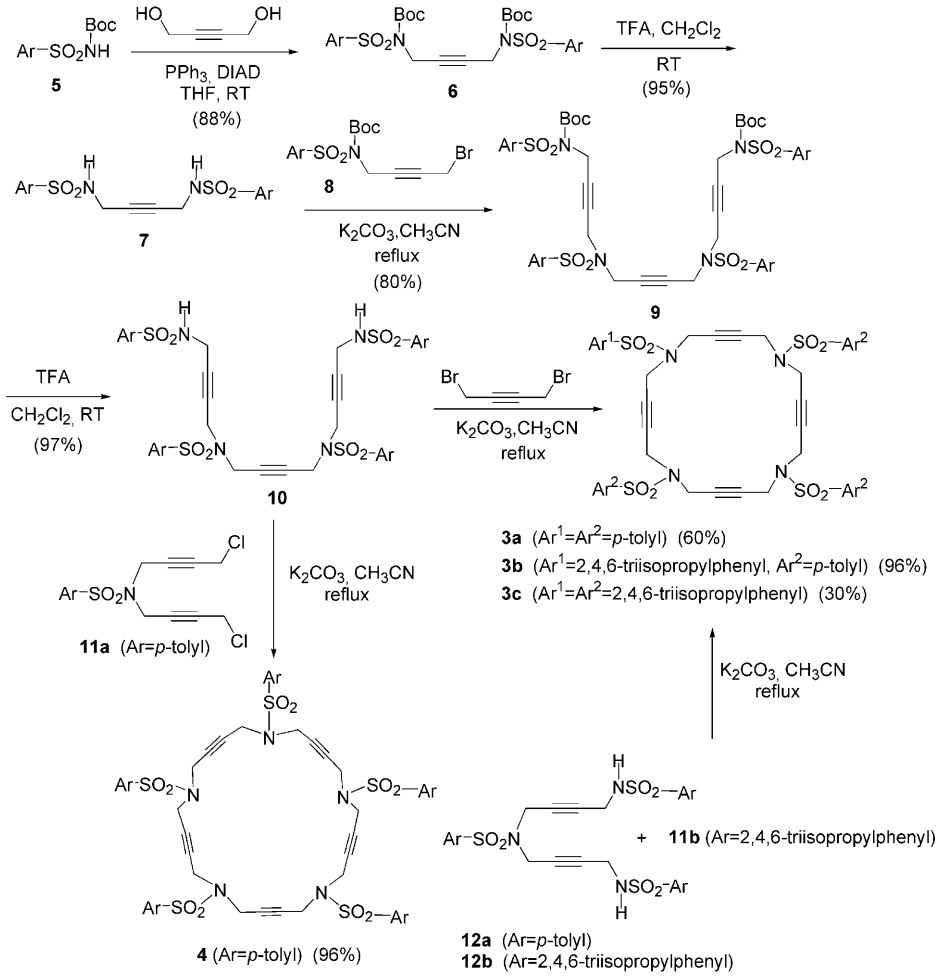

Scheme 2. Synthesis of acetylenic azamacrocycles **3a**, **3b**, **3c** and **4**.

After a pioneering semiempirical study,[9] several DFT investigations into the reaction mechanism of the transition-metal-catalysed [2+2+2] cyclotrimerisation reactions involving alkynes have been reported in the last decade. The reaction mechanism for the alkyne cyclotrimerisation reaction catalysed by $[CoCp(L)_2]$ (Cp = cyclopentadiene; L = CO, PR_3, THF and olefin),[10–13] [RuCpCl][14–17] complexes and the {RhCp}[18] and {RhInd} (Ind = indene)[18] fragments has been analysed in these DFT studies. The generally accepted reaction mechanism is drawn in Scheme 3. The reaction begins with a pair of ligand–alkyne substitution reactions. Then, the oxidative coupling of the two alkyne ligands generates a metallacyclopentadiene **IIIa** ($[CoCp(L)_2]$, {RhCp} and {RhInd}) or a metallacyclopentatriene **IIIb** ([RuCpCl]) with a biscarbene structure. This step has been found to be the rate-determining step with activation energies typically in the range 11–14 kcal mol^{-1}. Subsequent coordination of a third alkyne ligand to the metallacyclopentadiene or metallacyclopentatriene intermediate is followed by either alkyne insertion to form a planar aromatic metallacycloheptatriene **V** (the so-called Schore's mechanism[19]) or metal-mediated [4+2] cycloaddition to yield a 7-metallanorbornadiene complex **VI** or [2+2] cycloaddition to give a metallabicyclo [3.2.0]heptatriene **VII**. Finally, the arene is formed by the reductive elimination of the metal. Although this is the general picture of the reaction mechanism, differences are found between catalysts and the presence or absence of coordinating ligands, such as phosphine groups.[13]

On the other hand, the cyclotrimerisation of nitriles and acetylenes to afford pyridine rings has been also discussed in a series of theoretical studies.[17,18,20,21] The rate-determining step of the overall catalytic cycle changes to become the addition of the nitrile molecule to the metallacyclopentadiene or metallacyclopentatriene intermediate.[17,18] One of

Abstract in Catalan: *S'ha sintetitzat i caracteritzat espectroscòpicament una nova sèrie de macrocicles nitrogenats poliacetilènics de 20- i 25-membres. Amb aquests macrocicles s'han dut a terme les reaccions de ciclotrimerització [2+2+2] catalitzades pel catalitzador de Wilkinson, [RhCl(PPh$_3$)$_3$]. El macrocicle nitrogenat de 25-membres (de la mateixa manera que el macrocicle nitrogenat de 15-membres) permet l'obtenció del compost ciclotrimeritzat. Per contra, el macrocicle de 20-membres es caracteritza per la seva falta de reactivitat. El diferent comportament de reactivitat dels macrocicles de 15-, 20-, i 25-membres ha estat estudiat mitjançant càlculs teòrics basats en la teoria del funcional de la densitat.*

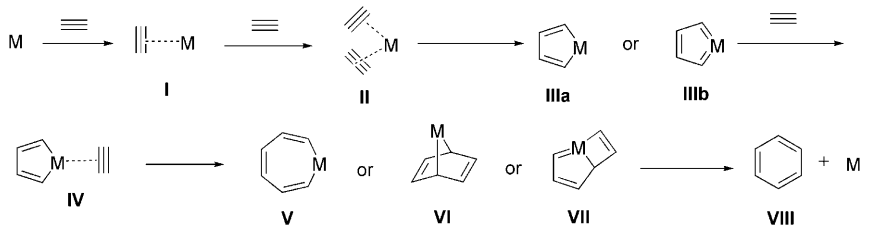

Scheme 3. Schematic [2+2+2] reaction mechanism with M = transition metal.

the key aspects in the cyclotrimerisation of nitriles and acetylenes is the competition between arene and pyridine formation. Relevant to our discussion are also several papers that address the co-cyclisation of two acetylene molecules with alkenes or CS_2.[14,22–25] Finally, we can briefly mention here that the uncatalysed thermal cyclotrimerisation is disfavoured entropically and has a high activation barrier.[26,27]

To the best of our knowledge, a theoretical study of the reaction mechanism of the transition-metal-catalysed [2+2+2] cyclotrimerisation reaction in a macrocyclic triyne has yet to be performed. This [2+2+2] reaction should be favoured over cyclotrimerisation reactions involving free acetylene molecules for entropic reasons.[15] In this paper we report the results of our theoretical examination of the mechanism for the cyclotrimerisation catalysed by the Wilkinson's complex of the 15-, 20- and 25-membered acetylenic azamacrocycles depicted in Scheme 4 with two main goals: 1) to investigate the origin for the different reactivity of the 20-membered tetraacetylenic azamacrocycles and 2) to discuss the chemoselectivity of the trimerisation in the case of the pentaacetylenic azamacrocycles for which more than a single product can be obtained as cycloaddition can occur between three adjacent or non-adjacent triple bonds. This is, we believe, the first theoretical study that addresses the mechanism of a cyclotrimerisation reaction in a series of acetylenic macrocycles. Furthermore, this is the first time that the Wilkinson's catalyst has been investigated in a theoretical study of an intramolecular cyclotrimerisation reaction.

Results and Discussion

Macrocycles **3** and **4** were prepared following the synthetic pathway outlined in Scheme 2 and they were completely characterised by spectroscopic methods (see Supporting Information for full experimental details). One of the variants these macrocycles can present is the nature of the aryl units of the periphery. Firstly, two macrocycles **3a** and **4** containing the same arylic unit, *p*-tolylsulfonamide, were prepared. The whole synthesis started with the reaction of *N-tert*-butyloxycarbonyl (Boc)-protected *p*-tolylsulfonamide **5**[28] and 0.5 equiv of 2-butyne-1,4-diol under Mitsunobu reaction conditions to give compound **6**. The elimination of the Boc groups in compound **6** (to give **7**) and the subsequent treatment with two equivalents of bromo derivative **8**[5] resulted

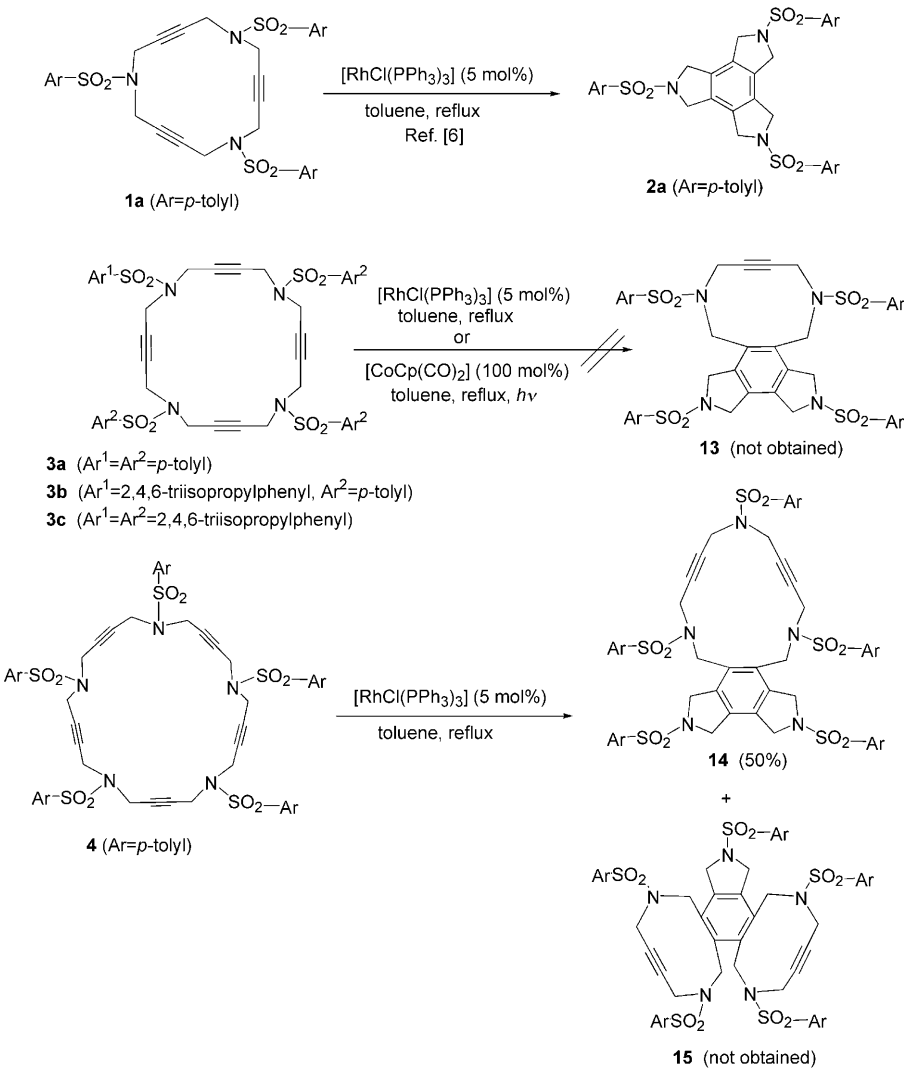

Scheme 4. Studies on cyclotrimerisation reactions of 15-,[6] 20- and 25-membered acetylenic azamacrocycles **1**, **3** and **4**.

in the isolation of compound **9** with an 80% yield. The elimination of the Boc groups again with the same reaction conditions as before (TFA in CH_2Cl_2) gave intermediate **10**. Compound **10**, which already contains three acetylenic chains and four sulfonamide units, was the key intermediate for the preparation of both macrocycles. Cyclisation of **10** with 1,4-dibromo-2-butyne in the presence of K_2CO_3 as a base afforded a 60% yield of macrocycle **3a**. When intermediate **10** was condensed with the dichloro derivative **11a**, previously prepared by us,[8] 25-membered pentaacetylenic macrocycle **4** was obtained with an almost quantitative yield. The *p*-tolylsulfonamide units give a high level of insolubility in the most common organic solvents in the 20-membered macrocycle. This permitted suitable crystals to be obtained to make X-ray diffraction analysis. Figure 1 shows the Ortep-plot diagram for the compound together with its labelling scheme. Compound **3a** crystallises free of solvent molecules with C_1 symmetry. Bond lengths and angles are within expected values. The four triple bonds at the macrocyclic ring are located on different planes.

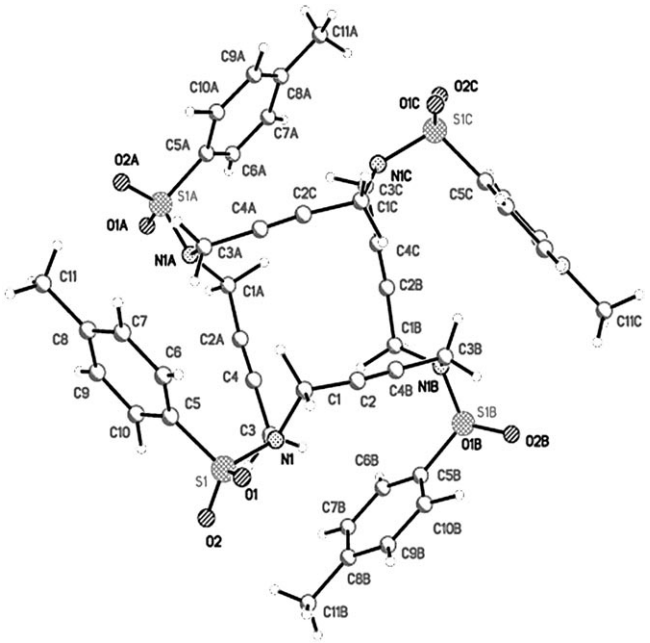

Figure 1. Ortep plot (50%) of macrocycle **3a**.

Given that macrocycle **3a** had a high level of insolubility we decided to prepare two macrocycles, **3b** and **3c**, containing units of 2,4,6-triisopropylphenyl in order to increase solubility. To introduce an arylic unit that was different to the other three and to prepare **3b**, an alternative synthetic route was used (see Scheme 2). Condensation between dichloro derivative **11b**,[8] which introduces the differential aryl unit, and trisulfonamide **12a**[6] afforded a 96% yield of macrocycle **3b**. Reaction of **12b**[6] with **11b**[8] gave macrocycle **3c** containing four units of 2,4,6-triisopropylphenyl.

After preparing the macrocycles, the next step was to study how to obtain fused tetracycles **13**–**15** by [2+2+2] cyclotrimerisation reactions. There is one possible way for macrocyles **3** to cyclise to afford a single 5,5,10-fused benzene derivative. However, in the case of the 25-membered ring **4** there are two possible ways of cyclisation; that is, cycloaddition between three consecutive triple bonds to afford compound **14** or between non-consecutive triple bonds to afford compound **15**. The Wilkinson's catalyst $[RhCl(PPh_3)_3]$ was selected as it had formerly given the best results in our previous studies.[5–8] When 20-membered macrocycles **3a**–**c**, heated under reflux in toluene, were treated with $[RhCl(PPh_3)_3]$, the reaction did not take place. In all three cases, starting material together with decomposition products were obtained. A stoichiometric amount of $[CpCo(CO)_2]$, another typical catalyst for this chemistry,[1–4] was also tested. The macrocycle was heated under reflux in toluene and the solution was exposed to light. However, this reaction also failed and the starting macrocycle was recovered. In contrast, when 25-membered macrocycle **4** was treated with a catalytical amount of rhodium complex, the cyclotrimerised compound **14**, resulting from the reaction of three contiguous alkynes, was obtained as the only product of the process. Confirmation of the structure of **14** was made by HMBC and 2D NOESY data (see the Supporting Information). Experimentally we observe that 5,5,15-fused core is more favourable than 5,10,10-fused system.

As stated in the Introduction section, we performed B3LYP/cc-pVDZ-PP calculations (see section on Computational Methods for a more detailed description of the method used) to unravel the reaction mechanism of the intramolecular [2+2+2] cyclotrimerisation catalysed by the Wilkinson's complex of the 15-, 20- and 25-membered acetylenic azamacrocycles (MAAs) depicted in Scheme 4 in order to understand the lack of reactivity of the 20-MAA. As we will see, these DFT computations turned out to be very helpful to rationalise the experimental outcome. To reduce the computational effort required, the SO_2-Ar moieties present in the experimental 15-, 20- and 25-MAA and the three Ph groups of the Wilkinson's catalyst were substituted by H atoms. Before starting our theoretical study, we checked that the thermodynamics of the **1a**→**2a** conversion is not significantly altered when going from the real system with the *p*-tolylsulfonamide units to the model system. Our results show that the **1a**→**2a** process in the real system is exothermic by $-140.3\ kcal\,mol^{-1}$ at the B3LYP/cc-pVDZ-PP level, while in our model system is found to be exothermic by $-128.4\ kcal\,mol^{-1}$. Thus, substitution of the SO_2-Ar moieties by H atoms reduces the exothermicity of the reaction by approximately 10%. Although this quantity is not negligible, we think that it affects similarly the different reactions studied and, therefore, the conclusions reached by comparison with our model systems should be still valid for the real systems.

We proceed now by examining the reaction mechanism for the 15-MAA. The energy profile of the $[RhCl(PH_3)_3]$-catalysed cyclotrimerisation of this 15-MAA is presented in

Figure 2. The *xyz* cartesian coordinates of all minima and transition states (TSs) can be found in the Supporting Information. As can be seen, initially the $[RhCl(PH_3)_3]$ complex

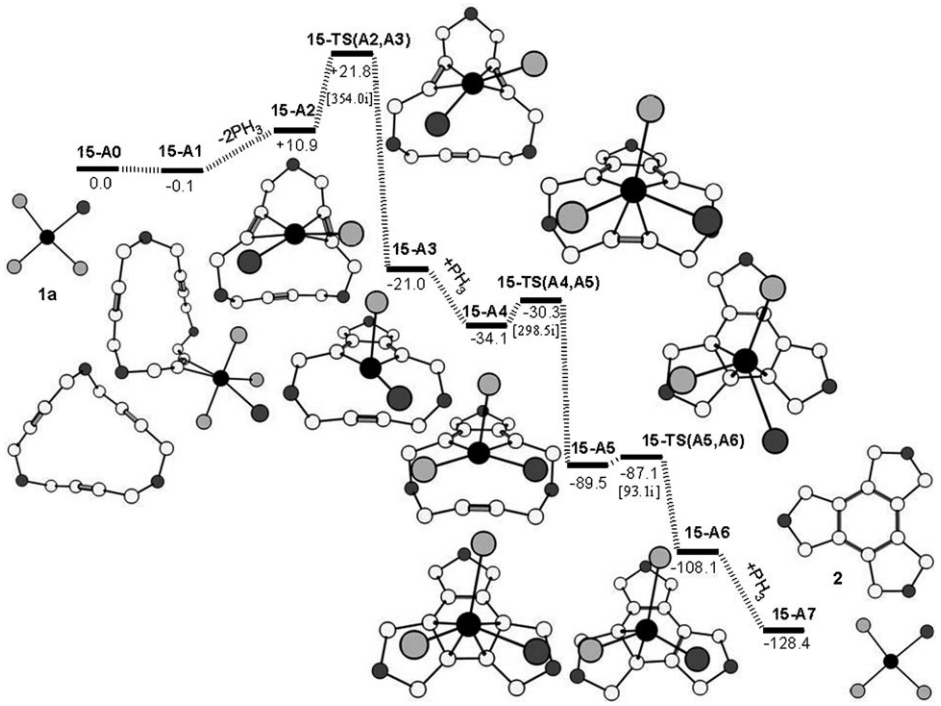

Figure 2. Reaction Gibbs free-energy profile for the [2+2+2] cyclotrimerisation of our model of macrocycle **1a**. Relative free-energy values in kcal mol^{-1}. Imaginary frequencies [cm^{-1}] for the different transition states are given in brackets. For the sake of clarity nonrelevant H atoms have been omitted.

10.9 kcal mol^{-1} and a Gibbs free-reaction energy of −31.9 kcal mol^{-1}. These values are in line with those obtained for the conversion of a bisacetylene [RuClCp] complex into a ruthenacyclopentatriene in three different studies of about 13 and −35 kcal mol^{-1}, respectively.[14,15,17] On the other hand, similar barriers but lower exothermicities were reported for RhCp and CoCp-catalysed cyclotrimerisations.[10,17,18] As found previously in similar Co and Rh complexes, the **15-A3** complex exhibits π localisation with C_α–C_β and C_β–$C_{\beta'}$ bond lengths of 1.351 and 1.453 Å, respectively, despite the presence of metal lone pairs that could favour the formation of an aromatic ring.[10,18] The Rh–C bond length of 2.04 Å is not far from the average crystallographic bond length of 2.01 Å.[18] The Rh–C bond lengths for the C atoms of the triple bond still present in this complex, suggest that the π-electronic structure interacts with the metal in an η^2 fashion in **15-A3**. This complex resembles the only reported example of a metalcyclopentadiene(alkyne) species determined by X-ray diffraction.[30] The organometallic complex **15-A3** shows a C_α–C_β bond length of 1.351 Å (to be compared with 1.358 Å in the reported metalcyclopentadiene(alkyne) system[30]), and a C_β–$C_{\beta'}$ bond length of 1.453 Å, almost identical to that previously reported.[30]

weakly interacts externally with a triple bond to form the 18-electron complex **15-A1**. After that, the distorted trigonal bypiramidal complex **15-A2** is generated by replacing two phosphines by two internal η^2 interactions with adjacent acetylenic units of the 15-MAA. This process is endoergonic by 10.9 kcal mol^{-1}, although this endoergonicity is probably overestimated as a result of the substitution of the PPh_3 ligands in the Wilkinson's catalyst by a stronger donor such as PH_3.[29] The substitution of the phosphines by acetylene units in the formation of **15-A2** can follow a dissociative or associative mechanism. Although we have not analysed this point in detail, we consider that because of the small cavity size in the 15-MAA, the associative mechanism is very unlikely. Next, the oxidative coupling of the two alkyne groups in **15-A2** leads to the distorted trigonal-bypiramidal bicyclorhodacyclopentadiene **15-A3**. The TS corresponding to this transformation is depicted in Figure 3.

The C_β–$C_{\beta'}$ distance of 1.948 Å is close to that found for the corresponding TS of the transformation of a 1,6-diyne into a similar ruthenabicyclo complex (2.040 Å).[15] On the other hand, a significant shortening of the Rh–C_α bond lengths is observed (from 2.247 to 2.078 Å), but the C_α–C_β bonds are only slightly elongated with respect to **15-A2**. The conversion of **15-A2** into **15-A3** is the rate-determining step of the overall process with a Gibbs free-energy barrier of

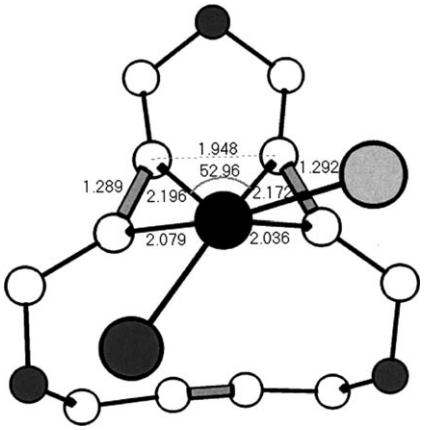

Figure 3. Optimised structure (B3LYP/cc-pVDZ-PP) for 15-TS(**A2**,**A3**) with the most relevant bond lengths [Å] and angles [°].

We have not investigated the possible formation of η^4-cyclobutadiene-like complexes as a result of a thermal cyclodimerisation from **15-A2**, because this process was found to be kinetically quite unfavourable in similar species.[31] The photochemical process instead is more favourable.[30] The 16-electron **15-A3** complex adds a phosphine molecule to yield the 18-electron species **15-A4** with a Gibbs free-energy stabilisation of 13.1 kcal mol^{-1}. The coordination of this PH_3 promotes an elongation from 2.033 to 2.076 Å of the bond length between the Rh and the C_α on the opposite side of this PH_3. The process that converts **15-A4** into **15-A5** is an intramolecular [4+2] cycloaddition of the coordinated alkyne of the 15-MAA to the rhodacyclopentadiene. This reaction has a small barrier of only 3.8 kcal mol^{-1} and is exoergonic by 55.4 kcal mol^{-1} in line with previous studies.[10,18] The driving force for this reaction comes from the formation of two new C–C σ-bonds and a partially aromatic distorted six-carbon arene ring.[10] The possible formation of rhodacycloheptatriene or 7-rhodanorbornadiene or rhodabicyclo [3.2.0]heptatriene intermediates was also investigated. None of these intermediates were located in our potential-energy surface for the 15-membered macrocycle. In the 18-electron **15-A5** complex the benzene formed ring is attached to the Rh^I through an η^4-interaction. The coordinated butadiene portion of the six-membered ring displays a significant short–long bond length alternation (BLA of 1.357/1.469 Å), which is an indication of the loss of ring aromaticity as compared to the free benzene ring and of the significant ring–metal interaction (both donation from the π system of the benzene ring to the metal and back-donation). This ring exhibits a hinge angle of 30°, similar to the 37° found by BLYP/TZ2P calculations in the [Rh(η^4-benzene)Cp] species[18] or the 42° measured in the X-ray structure of [Rh{η^5-$C_5(CH_3)_5$}{η^4-$C_6(CH_3)_6$}] complex.[32] The transformation from **15-A5** into distorted tetrahedral **15-A6** involves a ring slippage with a change of the arene-ring hapticity from η^4 to η^2. The barrier for this conversion is low (2.4 kcal mol^{-1}) and, somewhat unexpected when going from the 18- to 16-electron species, quite exoergonic by 18.6 kcal mol^{-1}. The thermodynamic driving force of this process is likely the partial recovery of aromaticity of the arene ring, which becomes planar and has a small BLA. Completion of the catalytic cycle occurs upon exoergonic (by 20.3 kcal mol^{-1}) displacement of the arene by a phosphine molecule to regenerate the [RhCl(PH_3)$_3$] catalyst.

Next, we examined the two possible reaction mechanisms for the [2+2+2] cyclotrimerisation catalysed by the [RhCl(PH_3)$_3$] complex in the 20-MAA. The Gibbs free-energy profile of this cyclotrimerisation is drawn in Figure 4.

The overall transformation is also very exoergonic (−122.0 kcal mol^{-1}), so the reason for the lack of reactivity of the 20-MAA must be kinetic. Although, the reaction

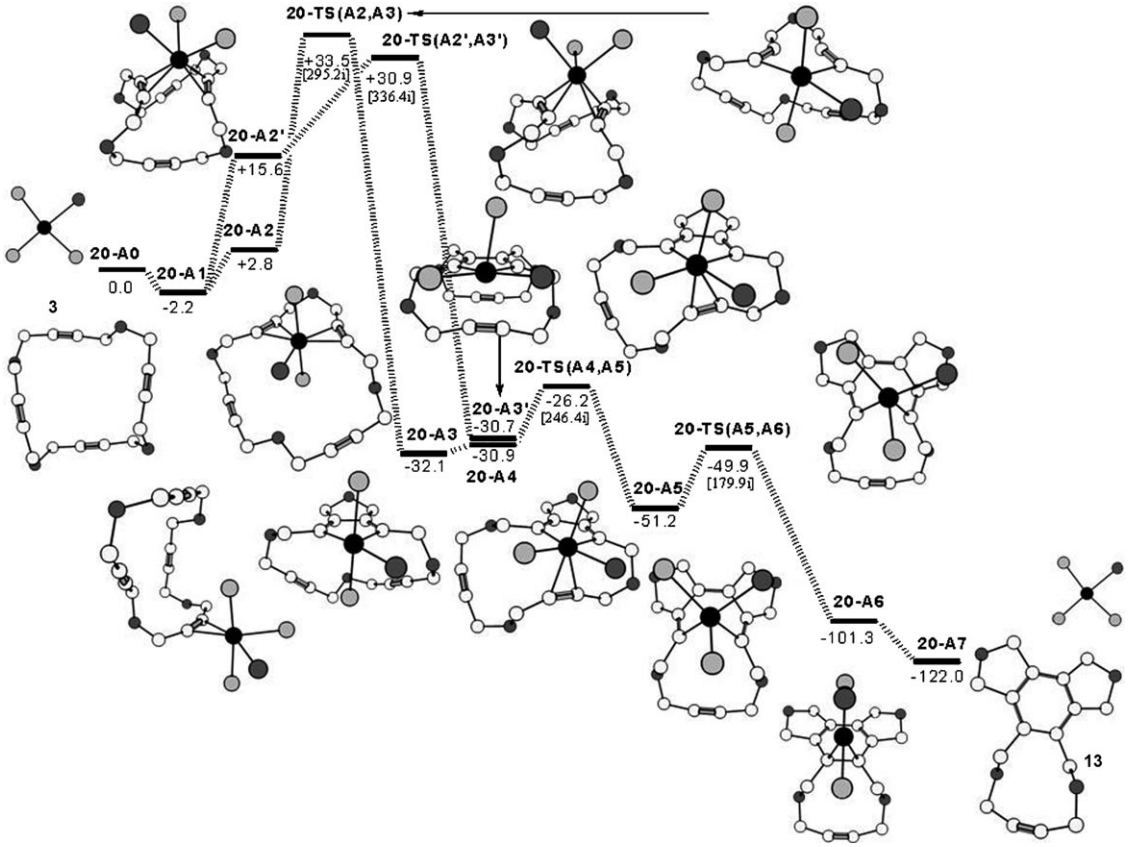

Figure 4. Reaction Gibbs free-energy profile for the [2+2+2] cyclotrimerisation of our model of macrocycle **3**. Relative free-energy values in kcal mol^{-1}. Imaginary frequencies [cm^{-1}] for the different transition states are given in brackets. For the sake of clarity nonrelevant H atoms have been omitted.

mechanism is similar to that found for the 15-MMA, there are three remarkable differences. First, 18-electron complex **20-A2** is generated by replacing a single (instead of two) phosphine ligand by two internal η^2 interactions with adjacent acetylenic units of the 20-MAA. This process is endoergonic by 2.8 kcal mol^{-1}. Second, there are two possible ways of coordinating two alkyne units in the macrocycle. Thus, species **20-A2′**, with two internal η^2 interactions with non-adjacent acetylenic units of the 20-MAA, can also be formed but it is less stable than **20-A2** by 12.8 kcal mol^{-1}. The conversion of **20-A2** and **20-A2′** into bicyclorhodacyclopentadiene **20-A3** and **20-A3′**, respectively, takes place by oxidative coupling of the two coordinated alkyne moieties through the TSs depicted in Figure 5 with Gibbs free-energy barriers of 30.7 and 15.3 kcal mol^{-1}, respectively. These values are clearly larger than those found for the same rate-determining step in the 15-MAA. The reasons for these higher energy barriers, which are in agreement with the experimental lack of formation of **13**, will be discussed later. Although the barrier for the transformation of **20-A2′** into **20-A3′** is lower than that for the equivalent **20-A2** into **20-A3** conversion, the two TSs differ by only 2.6 kcal mol^{-1} and we decided to continue the analysis of the reaction mechanism only from the **20-A3** species. The rearrangement converting **20-A3** into the distorted octahedral **20-A4** complex requires 3.6 kcal mol^{-1} and attaches one uncoordinated triple bond of the 20-MAA to the metal. Since no transition state connecting **20-A3** to **20-A4** was found, the barrier for this step is expected to be very low or absent. At this stage the third important difference arises. The process that transforms **20-A4** into **20-A5** is not a [4+2] cycloaddition, but rather a [2+2] asymmetric addition that results in the formation a non-planar rhodacycloheptatriene complex (see Figure 6) through the TS depicted in Figure 7. This process has a low barrier (4.7 kcal mol^{-1}) and is exoergonic by 20.3 kcal mol^{-1}. All attempts to find the TS corresponding to the [4+2] cycloaddition were unsuccessful. Thus, even small changes in the macrocycle can lead to important differences in the reaction mechanism of the [2+2+2] intramolecular cyclotrimerisation. A seven-membered ruthenacycle was also found in the reaction mechanism of the [2+2+2] cyclotrimerisation of alkynes.[15] Experimentally, the crystal structure of an iridacycloheptatriene with a tub-shaped conformation has been reported.[33] Our **20-A5** rhodacyclohepta-

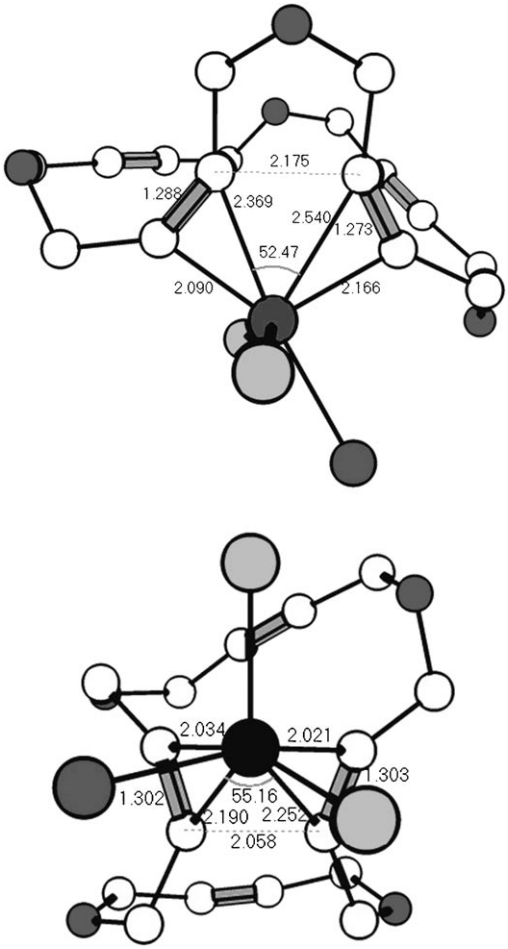

Figure 5. Optimised structures (B3LYP/cc-pVDZ-PP) for 20-TS(**A2**,**A3**) (top) and 20-TS(**A2′**,**A3′**) (bottom) with the most relevant bond lengths [Å] and angles [°].

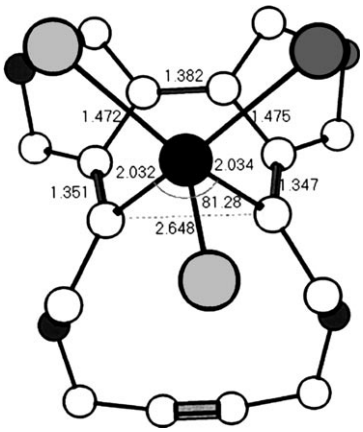

Figure 6. Optimised structure (B3LYP/cc-pVDZ-PP) for **20-A5** with the most relevant bond lengths [Å] and angles [°].

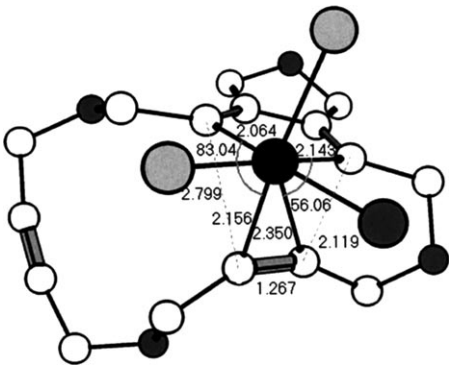

Figure 7. Optimised structure (B3LYP/cc-pVDZ-PP) for 20-TS(**A4**,**A5**) with the most relevant bond lengths [Å] and angles [°].

triene complex has a tub-shaped conformation with a short–long BLA of 1.347/1.475 Å similar to that found in the iridacycloheptatriene of 1.344/1.484 Å.[33] On the other hand, the bond length between the two carbons atoms not linked is 2.648 Å to be compared with the 2.885 Å found in the iridacycloheptatriene.[33] Final ring closure in **20-A5** provides **20-A6** in which the arene ring is coordinated in an η^2 fashion. The barrier for this reaction is only 1.3 kcal mol^{-1} and the exoergonicity is as large as 50.1 kcal mol^{-1}. Finally, the catalytic cycle is closed upon exoergonic displacement (by 20.7 kcal mol^{-1}) of the arene by a phosphine molecule to regenerate the $[RhCl(PH_3)_3]$ catalyst.

We shall now examine the reaction profile of the 25-MAA depicted in Figure 8. Due to the size of the 25-MAA, these calculations are extremely computationally demanding. For this reason, we only located the TSs corresponding to the first steps of the reaction mechanisms. As we have seen for the 15- and 20-MAA, the barriers involved in the last steps of the reaction mechanism are low and are expected to have little influence on the overall kinetics of the reaction. As shown in Scheme 4, there are two possible products (**14** and **15**) of the cyclotrimerisation of the 25-MAA. From a thermodynamic point of view, the reaction is favoured for the two products with exoergonicities of 121.6 and 98.8 kcal mol^{-1} for **14** and **15**, respectively. It is interesting, however, that the product experimentally observed is the most stable by 22.8 kcal mol^{-1}. It is likely that the greater stability of **14** relative to **15** is a result of the triple bonds in ten-membered rings being particularly strained. Indeed the $\measuredangle$CCC angle including the two carbon atoms linked by a triple bond is far from linear (around of 160° as compared to 179° in the 15-membered ring of **14**). This is in line with the fact that the exoergonicity of the trimerisation substantially decreases when going from the product of the 15-MAA (no ten-membered rings with triple bonds) to that of the 20-MAA (one ten-membered ring with triple bonds) to **15** (two ten-membered rings with triple bonds). Despite this, the thermodynamics alone cannot explain the formation of only **14**. As can be seen in Figure 8, 18-electron complexes **25-A2** and **25-A2′** are formed by replacing a single phosphine ligand by two internal η^2 interactions either with adjacent or non-adjacent acetylenic units of the 25-MAA. For the non-adjacent coordinated triple bonds species, the process is endoergonic by 13.5 kcal mol^{-1}. The subsequent oxidative coupling takes place through a very high Gibbs free-energy barrier of 52.9 kcal mol^{-1}. Therefore, this reaction pathway is inaccessible at the temperature of the reaction. Instead, coordination of two adjacent triple bonds requires only 2.3 kcal mol^{-1} and the barrier for the oxidative coupling to yield the rhodacyclopentadiene **25-A3** is low (of only 6.4 kcal mol^{-1}). The TSs for the transformation of **25-A2** into **25-A3** and **25-A2′** into **25-A3′** are depicted in Figure 9. We attribute the large barri-

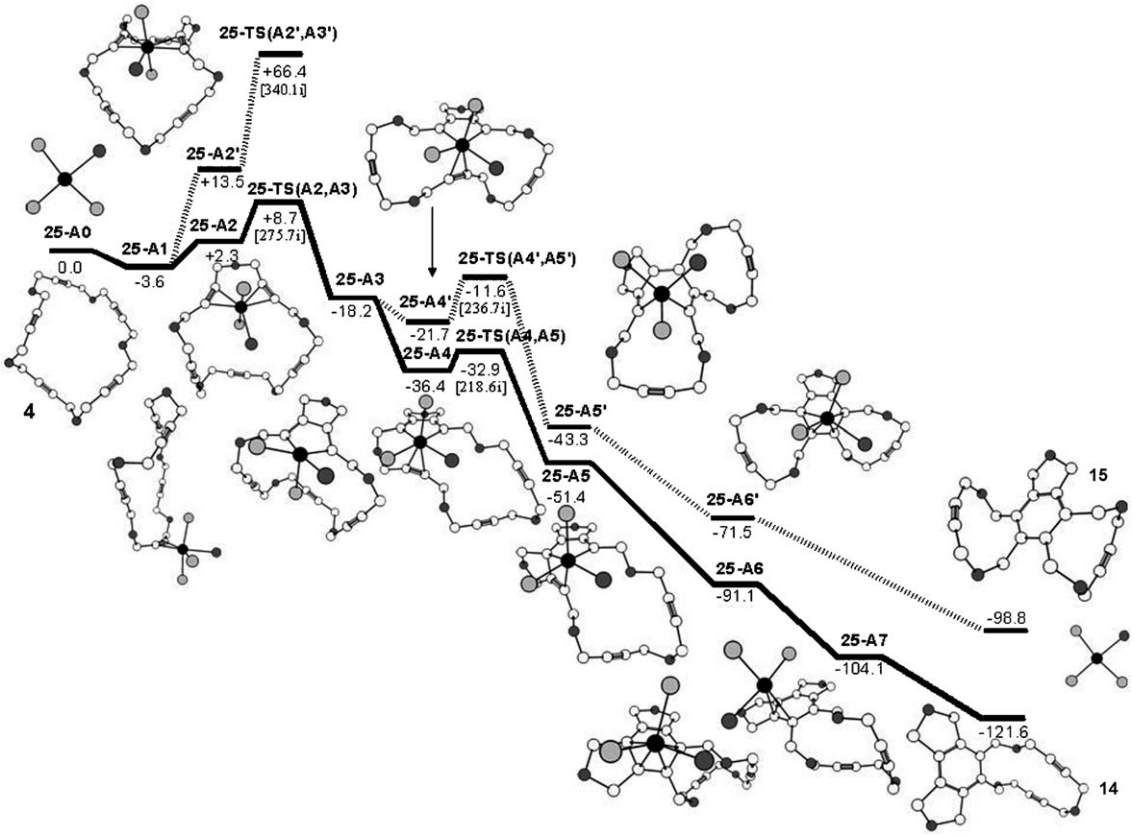

Figure 8. Reaction Gibbs free-energy profile for the [2+2+2] cyclotrimerisation of our model of macrocycle **4**. Relative free-energy values in kcal mol^{-1}. Imaginary frequencies [cm^{-1}] for the different transition states are given in brackets. For the sake of clarity nonrelevant H atoms have been omitted.

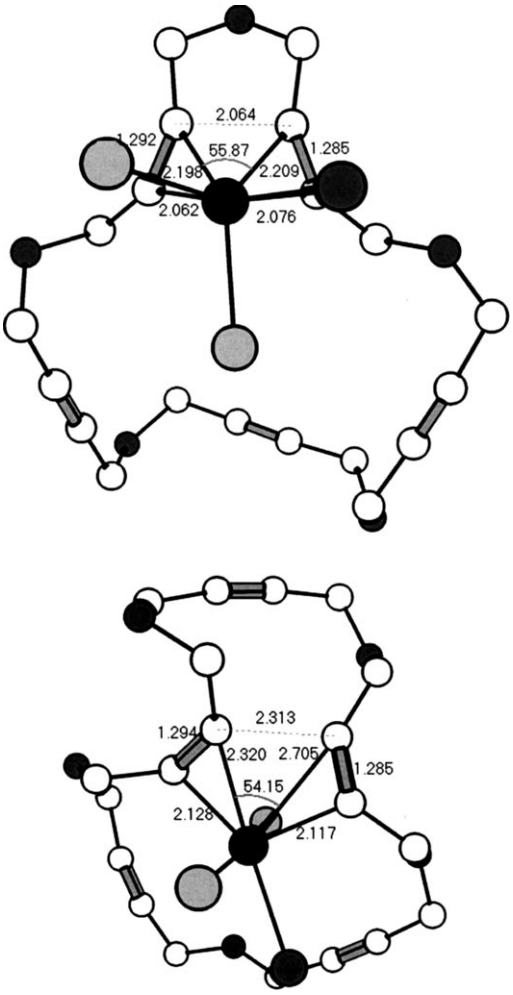

Figure 9. Optimised structure (B3LYP/cc-pVDZ-PP) for 25-TS(**A2**,**A3**) (top) and 25-TS(**A2′**,**A3′**) (bottom) with the most relevant bond lengths [Å] and angles [°].

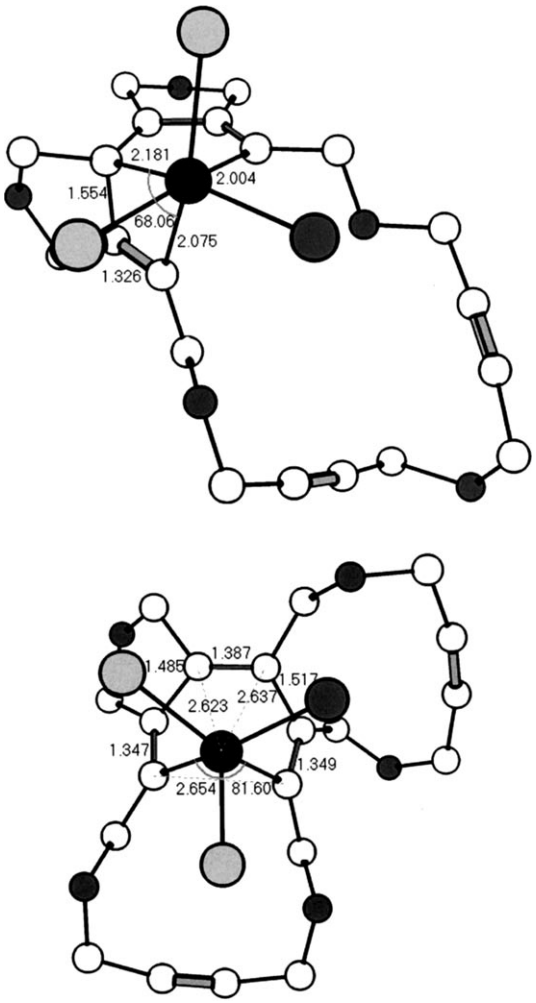

Figure 10. Optimised structure (B3LYP/cc-pVDZ-PP) for **25-A5** (top) and **25-A5′** (bottom) with the most relevant bond lengths [Å] and angles [°].

er found in the conversion of **25-A2′** into **25-A3′** in part to the deformation of the 20-MAA required in order to form two strained ten-membered rings. The deformation energy is 28.6 kcal mol^{-1} higher in the TS for the **25-A2′** into **25-A3′** than for the **25-A2** into **25-A3** transformation. Again in **25-A3** there are two possibilities for the coordination of a triple bond. The triple bond can be adjacent to those involved in the oxidative coupling that lead to the rhodacyclopentadiene **25-A3** or non-adjacent. In the former process, the complex **25-A4** is formed with a stabilisation of 18.2 kcal mol^{-1}, while in the latter the formation of the product **25-A4′** releases only 3.5 kcal mol^{-1}. In addition, the subsequent [2+2] cycloaddition to form the rhodacycloheptatriene complexes **25-A5** and **25-A5′** depicted in Figure 10 through the corresponding TSs (see Figure 11) is favoured in the case of the adjacent triple bond (Gibbs free-energy barrier of 3.5 kcal mol^{-1} with respect to 10.1 kcal mol^{-1} for the non-adjacent triple bond). Therefore, the reaction pathway involving addition of the three contiguous triple bonds is favoured, which explains the experimental formation of **14** and not of **15**. Final ring closure in **25-A5** provides **25-A6** in which the arene ring is coordinated in an η^4 fashion. Conversion of **25-A6** into **25-A7** occurs after ring slippage and final displacement of the arene by a phosphine molecule regenerates the $[RhCl(PH_3)_3]$ catalyst.

As reported in previous studies,[10–18] we have also found that the rate-determining step in the [2+2+2] cyclotrimerisation of ethynes is the initial oxidative coupling to yield the metallacyclopentadiene or metallacyclopentatriene intermediate. The Gibbs free-energy barriers obtained for this process in the 15-, 20- and 25-MAA are calculated to be 21.8, 30.9 and 8.7 kcal mol^{-1} with respect to separated reactants. The values obtained are in line with the experimental observations. To investigate the origin of the barriers, we divided the energy difference between the TS and the separated reactants into deformation energy and interaction energy (ΔE_{def}+ΔE_{int}). The deformation energy (ΔE_{def}) is the energy needed to modify the geometry of the free reactants to attain the geometry they have in the TS. The interaction energy (ΔE_{int}) is the energy released when the two free de-

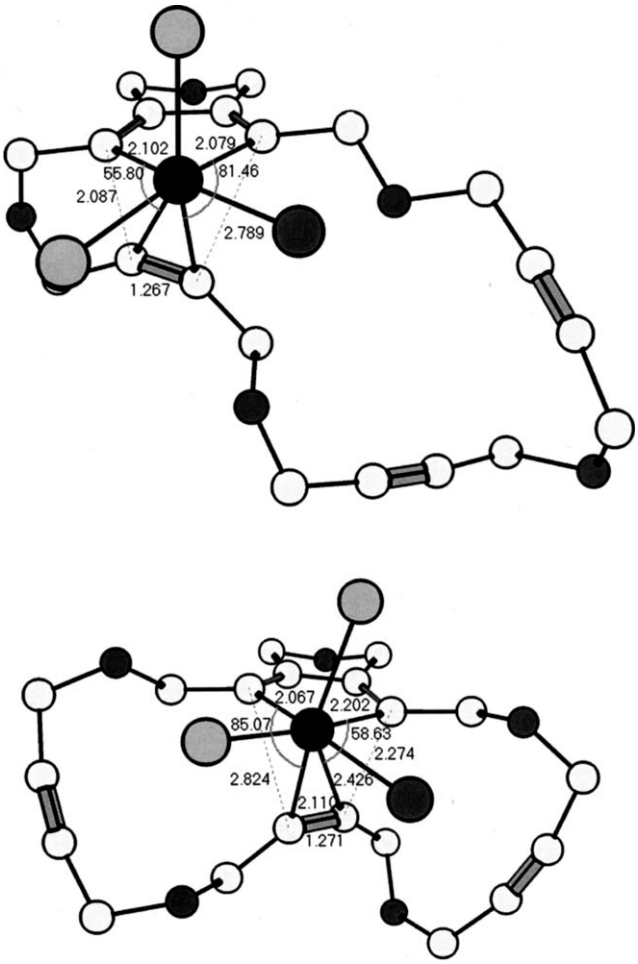

Figure 11. Optimised structure (B3LYP/cc-pVDZ-pp) for 25-TS(**A4**,**A5**) (top) and 25-TS(**A4′**,**A5′**) (bottom) with the most relevant bond lengths [Å] and angles [°].

formed reactants are brought to the position that they have in the TS. The calculated deformation energies for the 20- and 25-TS(**A2**,**A3**) are 95.9 and 104.4 kcal mol^{-1}, respectively. We have not included the 15-TS(**A2**,**A3**) in the analysis as the different number of phosphine ligands hamper the comparison. Clearly, the deformation energy in the TS is not the origin of the larger barrier for the 20-TS(**A2**,**A3**). The interaction energies are in turn −62.4 and −95.7 kcal mol^{-1} for the 20- and 25-TS(**A2**,**A3**), respectively. The main interaction in TS(**A2**,**A3**) occurs between the LUMO of the catalyst and the HOMO of the macrocycle. By comparing the HOMO and LUMO energies involved in the 20- and 25-TS(**A2**,**A3**), it can be seen that the main difference is the energy of the HOMO of the 20-MAA (−0.192 au) as compared to that of the 25-MAA (−0.172 au.). The HOMO–LUMO overlaps are quite similar in the two cases. A picture of the two HOMOs is given in Figure 12, showing a higher delocalisation of the HOMO in the deformed 20-MAA, which apparently is responsible for its greater stabilisation and, as a consequence, its lower reactivity. So, we concluded that the two factors that make the 20-MAA less reactive are

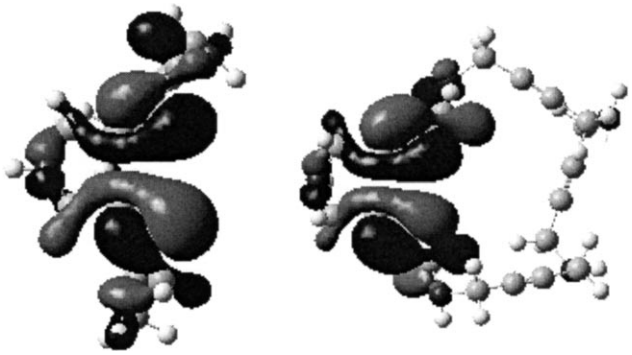

Figure 12. 3D-representation of the HOMOs for the 20- (left) and 25-MAA (right) at the geometry the macrocycles have in the 20- and 25-TS(**A2**,**A3**). Isosurface values are ±0.192 and ±0.172 au, respectively.

1) a more stable and delocalised HOMO orbital and 2) the formation of a strained ten-membered ring.

Conclusions

In summary, we report an efficient stepwise preparation of 20- and 25-membered macrocycles featuring four and five triple bonds, respectively, with different arylsulfonyl moieties in their structure. All new compounds are completely characterised by spectroscopic methods and additional evidence for structure was secured by X-ray diffraction for **3a**. An efficient rhodium(I)-catalysed [2+2+2] cyclotrimerisation of 25-membered pentaacetylenic azamacrocycle **4** chemoselectively afforded the cyclotrimerised compound **14** resulting from the reaction of three adjacent alkynes instead of the cyclotrimerisation between non-adjacent triple bonds. In contrast, the 20-membered tetraacetylenic azamacrocycles **3** did not lead to the expected cyclotrimerised compounds. DFT calculations to unravel the reaction mechanism of the 15-, 20- and 25-MAA revealed that there are two main factors that contribute to the lack of reactivity of the 20-MAA: 1) the 20-MAA has a more stable and delocalised HOMO orbital and 2) the formation of a strained ten-membered ring during the cyclotrimerisation of the 20-MAA. These two factors increase the free-energy barriers of the rate-determining step and difficult the intramolecular cyclotrimerisation of the 20-MAA.

Experimental Section

[2+2+2] Cyclotrimerisation of macrocycle 4: A degassed solution of macrocycle **4** (0.05 g, 0.045 mmol) and chlorotris(triphenylphosphane)-rhodium(I) (0.0020 g, 0.0022 mmol) in anhydrous toluene (10 mL) was heated under reflux for 30 h (TLC monitoring). The solvent was then evaporated and the residue was purified by column chromatography on silica gel with dichloromethane/ethyl acetate (20:1) to afford **14** (0.025 g, 50%) as a colourless solid. M.p. 194–196 °C; ^{1}H NMR (500 MHz, $CDCl_3$, 25 °C, TMS): δ = 2.40 (s, 12H), 2.45 (s, 6H), 3.59 (s, 4H), 3.72 (s, 4H), 4.14 (s, 4H), 4.33 (s, 4H), 4.48 (s, 4H), 7.15 (AA′BB′ system, J = 8.0 Hz, 4H), 7.35–7.38 (m, 10H), 7.63 (AA′BB′ system, J = 8.2 Hz, 2H),

7.78 ppm (AA′BB′ system, $J=8.2$ Hz, 4H); ^{13}C NMR (50 MHz, $CDCl_3$, 25 °C, TMS): $\delta=22.2$, 22.3, 37.6, 37.7, 45.8, 52.5, 53.8, 80.4, 80.6, 128.2, 128.4, 129.6, 130.1, 130.4, 130.6, 132.2, 134.0, 135.1, 136.2, 138.6, 144.7, 145.0, 145.3 ppm; IR $\tilde{\nu}=2923$, 1335, 1157 cm^{-1}; MS (MALDI-TOF: m/z: 1106 $[M+H]^+$, 1128 $[M+Na]^+$, 1144 $[M+K]^+$; elemental analysis calcd (%) for $C_{55}H_{55}N_5O_{10}S_5$.EtOAc (1194.495): C 59.33, H 5.32, N, 5.86; found: C 59.14 and 59.10, H 5.21 and 5.26, N 6.18 and 6.21.

X-ray data for 3a: CCDC-707902 (**3a**) contains the supplementary crystallographic data for this paper. These data can be obtained free of charge from The Cambridge Crystallographic Data Centre via www.ccdc.cam.ac.uk/data_request/cif.

Computational methods: All geometry optimisations were performed by using the hybrid DFT B3LYP[34–36] method with the Gaussian 03[37] program package. The geometry optimisations were performed without symmetry constraints. Analytical Hessians were computed to determine the nature of stationary points (one or zero imaginary frequencies for transition states and minima, respectively) and to calculate unscaled zero-point energies (ZPEs) as well as thermal corrections and entropy effects by using the standard statistical-mechanics relationships for an ideal gas.[38] These last two terms were computed at 298.15 K and 1 atm to provide the reported relative Gibbs free energies (ΔG_{298}). Furthermore, the connectivity between stationary points was established by intrinsic reaction path[39] calculations. The all-electron cc-pVDZ basis set was used for P, O, N, C and H atoms,[40,41] while for Rh we employed the cc-pVDZ-PP basis set,[42] containing an effective core relativistic pseudopotential. Relative energies were computed taking into account the total number of molecules present. The SO_2-Ar moieties present in the experimental 15-, 20- and 25-membered acetylenic azamacrocycles and the Ph group in the catalyst were substituted by H atoms to reduce the computational complexity of the calculations involving these ligands. Substitution of PPh_3 by PH_3 is a common procedure in theoretical organometallic chemistry.[10,31,43–47] In addition, we have checked that, despite the electronic and steric differences, substitution of PPh_3 by PH_3 does not introduce significant changes in the thermodynamics and kinetics of the cyclotrimerisation of three acetylene molecules.[48] A previous study found that solvent effects due to toluene and acetonitrile in [2+2+2] cyclotrimerisations are minor, likely due to the absence of charged or polarised intermediates and transition states in the reaction mechanism.[18] Because the reactions studied are carried out in toluene, solvent effects have not been included in the present calculations. Finally, since there is no experimental data suggesting the presence of paramagnetic intermediates, our studies were limited to the singlet-spin potential-energy surfaces. However, we did calculations for the triplet form of several intermediates and they were found always higher in energy than the singlet counterparts.

Acknowledgements

We would like to thank the Spanish MEC (projects CTQ2005-04968-C02-02/BQU; CTQ2005-08797-C02-01/BQU; CTQ2008-03077/BQU; CTQ2008-05409-C02-02/BQU; CTQ2006-01080) and the Catalan DURSI (projects 2005SGR-00238; 2005SGR-00305) for their financial support. A.D. and S.O. thank the Spanish MEC for a doctoral fellowship. We also acknowledge the Centre de Supercomputació de Catalunya (CESCA) for partial funding of computer time. We thank the Research Technical Services of the UdG for spectral data, especially Xavier Fontrodona for X-ray diffraction analysis.

[1] P. R. Chopade, J. Louie, *Adv. Synth. Catal.* **2006**, *348*, 2307–2327.
[2] V. Gandon, C. Aubert, M. Malacria, *Chem. Commun.* **2006**, 2209–2217.
[3] Y. Yamamoto, *Curr. Org. Chem.* **2005**, *9*, 503–519.
[4] S. Kotha, E. Brahmachary, K. Lahiri, *Eur. J. Org. Chem.* **2005**, 4741–4767.
[5] A. Pla-Quintana, A. Roglans, A. Torrent, M. Moreno-Mañas, J. Benet-Buchholz, *Organometallics* **2004**, *23*, 2762–2767.
[6] A. Torrent, I. González, A. Pla-Quintana, A. Roglans, M. Moreno-Mañas, T. Parella, J. Benet-Buchholz, *J. Org. Chem.* **2005**, *70*, 2033–2041.
[7] I. González, S. Bouquillon, A. Roglans, J. Muzart, *Tetrahedron Lett.* **2007**, *48*, 6425–6428.
[8] S. Brun, L. Garcia, I. González, A. Torrent, A. Dachs, A. Pla-Quintana, T. Parella, A. Roglans, *Chem. Commun.* **2008**, 4339–4341.
[9] C. Bianchini, K. G. Caulton, C. Chardon, M.-L. Doublet, O. Eisenstein, S. A. Jackson, T. J. Johnson, A. Meli, M. Peruzzini, W. E. Streib, A. Vacca, F. Vizza, *Organometallics* **1994**, *13*, 2010–2023.
[10] J. H. Hardesty, J. B. Koerner, T. A. Albright, G.-Y. Lee, *J. Am. Chem. Soc.* **1999**, *121*, 6055–6067.
[11] A. A. Dahy, N. Koga, *Bull. Chem. Soc. Jpn.* **2005**, *78*, 781–791.
[12] A. A. Dahy, C. H. Suresh, N. Koga, *Bull. Chem. Soc. Jpn.* **2005**, *78*, 792–803.
[13] N. Agenet, V. Gandon, K. P. C. Vollhardt, M. Malacria, C. Aubert, *J. Am. Chem. Soc.* **2007**, *129*, 8860–8871.
[14] K. Kirchner, M. J. Calhorda, R. Schmid, L. F. Veiros, *J. Am. Chem. Soc.* **2003**, *125*, 11721–11729.
[15] Y. Yamamoto, T. Arakawa, R. Ogawa, K. Itoh, *J. Am. Chem. Soc.* **2003**, *125*, 12143–12160.
[16] R. Schmid, K. Kirchner, *Eur. J. Inorg. Chem.* **2004**, 2609–2626.
[17] G. Dazinger, M. Torres-Rodrigues, K. Kirchner, M. J. Calhorda, P. J. Costa, *J. Organomet. Chem.* **2006**, *691*, 4434–4445.
[18] L. Orian, J. N. P. van Stralen, F. M. Bickelhaupt, *Organometallics* **2007**, *26*, 3816–3830.
[19] N. E. Schore, *Chem. Rev.* **1988**, *88*, 1081–1119.
[20] Y. Yamamoto, K. Kinpara, T. Saigoku, H. Takagishi, S. Okuda, H. Nishiyama, K. Itoh, *J. Am. Chem. Soc.* **2005**, *127*, 605–613.
[21] Y. Yamamoto, R. Ogawa, K. Itoh, *J. Am. Chem. Soc.* **2001**, *123*, 6189–6190.
[22] J. A. Varela, S. G. Rubín, L. Castedo, C. Saá, *J. Org. Chem.* **2008**, *73*, 1320–1332.
[23] V. Gandon, N. Agenet, K. P. C. Vollhardt, M. Malacria, C. Aubert, *J. Am. Chem. Soc.* **2006**, *128*, 8509–8520.
[24] M. M. Montero-Campillo, J. Rodríguez-Otero, E. Cabaleiro-Lago, *J. Phys. Chem. A* **2008**, *112*, 2423–2427.
[25] J. Rodríguez-Otero, M. M. Montero-Campillo, E. Cabaleiro-Lago, *J. Phys. Chem. A* **2008**, *112*, 8116–8120.
[26] A. Ioffe, S. Shaik, *J. Chem. Soc. Perkin Trans. 2* **1992**, 2101–2108.
[27] R. D. Bach, G. J. Wolber, H. B. Schlegel, *J. Am. Chem. Soc.* **1985**, *107*, 2837–2841.
[28] B. R. Neustadt, *Tetrahedron Lett.* **1994**, *35*, 379–380.
[29] Indeed, at the same level of theory, substitution of two phosphine ligands by acetylene molecules in $[RhCl(PPh_3)_3]$ is exoergonic by about 12 kcal mol^{-1}, while in $[RhCl(PH_3)_3]$ it is exoergonic but by only 0.3 kcal mol^{-1} (A. Dachs, S. Osuna, A. Roglans, M. Solà, unpublished results).
[30] P. I. Dosa, G. D. Whitener, K. P. C. Vollhardt, A. D. Bond, S. J. Teat, *Org. Lett.* **2002**, *4*, 2075–2078.
[31] L. F. Veiros, G. Dazinger, K. Kirchner, M. J. Calhorda, R. Schmid, *Chem. Eur. J.* **2004**, *10*, 5860–5870.
[32] W. J. Bowyer, J. W. Merkert, W. E. Geiger, A. L. Rheingold, *Organometallics* **1989**, *8*, 191–198.
[33] E. Álvarez, M. Gómez, M. Paneque, C. M. Posadas, M. L. Poveda, N. Rendón, L. L. Santos, S. Rojas-Lima, V. Salazar, K. Mereiter, C. Ruiz, *J. Am. Chem. Soc.* **2003**, *125*, 1478–1479.
[34] A. D. Becke, *J. Chem. Phys.* **1993**, *98*, 5648–5652.
[35] C. Lee, W. Yang, R. G. Parr, *Phys. Rev. B* **1988**, *37*, 785–789.
[36] P. J. Stephens, F. J. Devlin, C. F. Chabalowski, M. J. Frisch, *J. Phys. Chem.* **1994**, *98*, 11623–11627.
[37] Gaussian 03, Revision C.01, M. J. Frisch, G. W. Trucks, H. B. Schlegel, G. E. Scuseria, M. A. Robb, J. R. Cheeseman, J. A. Montgomery, Jr., T. Vreven, K. N. Kudin, J. C. Burant, J. M. Millam, S. S. Iyengar, J. Tomasi, V. Barone, B. Mennucci, M. Cossi, G. Scalmani, N. Rega, G. A. Petersson, H. Nakatsuji, M. Hada, M. Ehara, K. Toyota, R. Fukuda, J. Hasegawa, M. Ishida, T. Nakajima, Y. Honda, O. Kitao, H. Nakai, M. Klene, X. Li, J. E. Knox, H. P. Hratchian, J. B. Cross, V. Bakken, C. Adamo, J. Jaramillo, R. Gomperts, R. E.

Stratmann, O. Yazyev, A. J. Austin, R. Cammi, C. Pomelli, J. W. Ochterski, P. Y. Ayala, K. Morokuma, G. A. Voth, P. Salvador, J. J. Dannenberg, V. G. Zakrzewski, S. Dapprich, A. D. Daniels, M. C. Strain, O. Farkas, D. K. Malick, A. D. Rabuck, K. Raghavachari, J. B. Foresman, J. V. Ortiz, Q. Cui, A. G. Baboul, S. Clifford, J. Cioslowski, B. B. Stefanov, G. Liu, A. Liashenko, P. Piskorz, I. Komaromi, R. L. Martin, D. J. Fox, T. Keith, M. A. Al-Laham, C. Y. Peng, A. Nanayakkara, M. Challacombe, P. M. W. Gill, B. Johnson, W. Chen, M. W. Wong, C. Gonzalez, J. A. Pople, Gaussian, Inc., Wallingford CT, **2004**.

[38] P. Atkins, J. De Paula in *Physical Chemistry*, Oxford University Press, Oxford, **2006**.

[39] C. Gonzalez, H. B. Schlegel, *J. Chem. Phys.* **1989**, *90*, 2154–2161.

[40] T. H. Dunning, Jr., *J. Chem. Phys.* **1989**, *90*, 1007–1023.

[41] D. E. Woon, T. H. Dunning, Jr., *J. Chem. Phys.* **1993**, *98*, 1358–1371.

[42] K. A. Peterson, D. Figgen, M. Dolg, H. Stoll, *J. Chem. Phys.* **2007**, *126*, 124101.

[43] Q. Cui, D. G. Musaev, K. Morokuma, *Organometallics* **1997**, *16*, 1355–1364.

[44] Q. Cui, D. G. Musaev, K. Morokuma, *Organometallics* **1998**, *17*, 742–751.

[45] Q. Cui, D. G. Musaev, K. Morokuma, *Organometallics* **1998**, *17*, 1383–1392.

[46] W. Zheng, A. Ariafard, Z. Lin, *Organometallics* **2008**, *27*, 246–253.

[47] Y. Abe, K. Kuramoto, M. Ehara, H. Nakatsuji, M. Suginome, M. Murakami, Y. Ito, *Organometallics* **2008**, *27*, 1736–1742.

[48] For the cyclotrimerisation of three acetylene molecules catalysed by $[RhCl(PR_3)_3]$, the reaction energy is $-165.2\ kcal\,mol^{-1}$ for both R = H and Ph_3, while the energy barrier for the rate-determining step is 11.9 and 12.9 $kcal\,mol^{-1}$ for R = H and Ph_3, respectively (A. Dachs, S. Osuna, A. Roglans, M. Solà, unpublished results).

Received: December 5, 2008
Published online: April 22, 2009

